Journal of Medicinal Chemistry

pubs.acs.org/jmc

Article

Efficient Silencing of Androgen Receptor Gene via UTR-Targeting siRNAs for Androgenetic Alopecia Therapy

Di Feng,[#] Xinli Fan,[#] Yuqiang Hu,[#] Yizhi Man, Qian Wang, Yanmin Song, Jingjing Zhou, Jin Zhang, Yun Luo, Jing Wang,[*] and Xinjing Tang[*]

Cite This: *J. Med. Chem.* 2025, 68, 20586−20594

Read Online

ACCESS | Metrics & More | Article Recommendations | Supporting Information

ABSTRACT: Androgenetic alopecia (AGA) is predominantly driven by excessive local activity of dihydrotestosterone (DHT), leading to follicular miniaturization and progressive hair loss. The need for novel treatment strategies for AGA is emphasized by the side effects and postoperative sequelae of current therapeutic approaches, including pharmacological interventions and surgical procedures. Small-interfering RNAs (siRNAs) have emerged as promising therapeutic candidates due to their target specificity, the enhanced efficacy, and long-term effect. Here, we screened a series of siRNA sequences targeting non-coding region of androgen receptor (AR) gene and identified a lead siRNA candidate (AR-27) conserved between*Homo sapiens* and*Mus musculus*. The chemically modified and cholesterol-conjugated candidate (AR-27 E-Chol) was evaluated in both cells and DHT-induced AGA mice model. AR-27 E-Chol effectively stimulated dorsal hair regrowth and significantly downregulated AR gene expression in skin tissues. These findings support the clinical potential of AR-27 E-Chol as an effective therapeutic candidate for AGA.

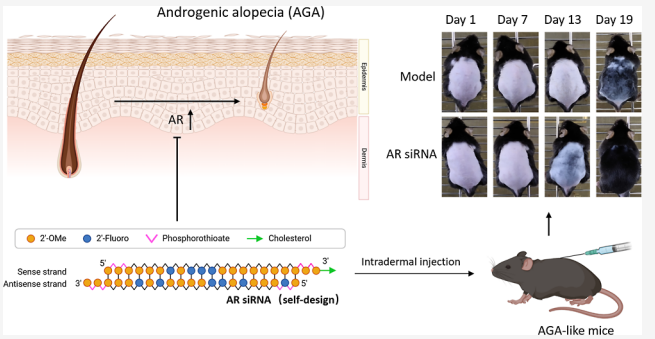

INTRODUCTIONS

Androgenetic alopecia (AGA), clinically referred to as premature baldness or seborrheic alopecia, is a progressively prevalent condition affecting both males and females. Common symptoms of AGA include hair pigmentation, the presence of vellus hair, peripilar signs around hair roots, and variability in hair shaft diameter.[1] The basic and special types (BASP) classification was proposed in 2007[2] and modified in 2020[3] to provide a systematic and universal classification for clinical hair loss gratification of AGA. Although AGA is not life-threatening, it significantly impairs life quality and mental health of patients due to the long-term severe anxiety and distress caused by deficient appearance.[4] Although the detailed mechanism of AGA is unclear so far, many studies indicate that AGA is mainly induced by genetic factors and endocrine factors, such as androgen disorder, inflammation around hair follicles, excessive mental stress, and unhealthy lifestyle.[5] Especially, high level of dihydrotestosterone (DHT) accumulates locally around the dermal papilla cells (DP) in dermis, leading to the transformation of normal hair follicles to susceptible follicles, followed by hair follicles miniaturization, shortened anagen, and stagnant telogen.[6,7] Clinical data confirm that androgen receptor (AR) gene is overexpressed in AGA patients and is closely associated with the occurrence and progression of hair loss,[8,9] indicating its critical role in the AGA pathogenesis and its potential as a therapeutic target for AGA.

Currently approved drugs for AGA are minoxidil and finasteride, as designated by the Food and Drug Administration (FDA). Minoxidil was first used to lower blood pressure to dilate blood vessels of scalp and stimulate the proliferation and differentiation of hair follicles.[10] However, the side effects such as contact dermatitis and facial hypertrichosis limit the applications of minoxidil.[11] Finasteride inhibits 5α-reductase to reduce the conversion of testosterone to DHT,[12] which can partially alleviate AGA. However, serious side effects in reproductive system and mental disease[13] were unavoidable. Therapeutic antibodies have been reported for AGA treatment through targeting PRLR,[14] IL-6R,[15] CXCL12,[16] and DKK1.[17] Although AR is directly involved in AGA pathogenesis, there is no AR-targeting antibody for AGA treatment,[18] probably due to the similar side effects as small molecule drugs like finasteride. Additionally, antibody administration might trigger a robust immunogenic response, making it a challenge to antibody-based therapy for AGA.[19] With the development of gene therapy, functional nucleic acid drugs such as small-interfering RNA (siRNA),[20] ASO,[21] aptamers,[22] and mRNA[23]

Received: June 29, 2025
Revised: August 27, 2025
Accepted: September 19, 2025
Published: September 26, 2025

https://doi.org/10.1021/acs.jmedchem.5c01739
J. Med. Chem. 2025, 68, 20586−20594

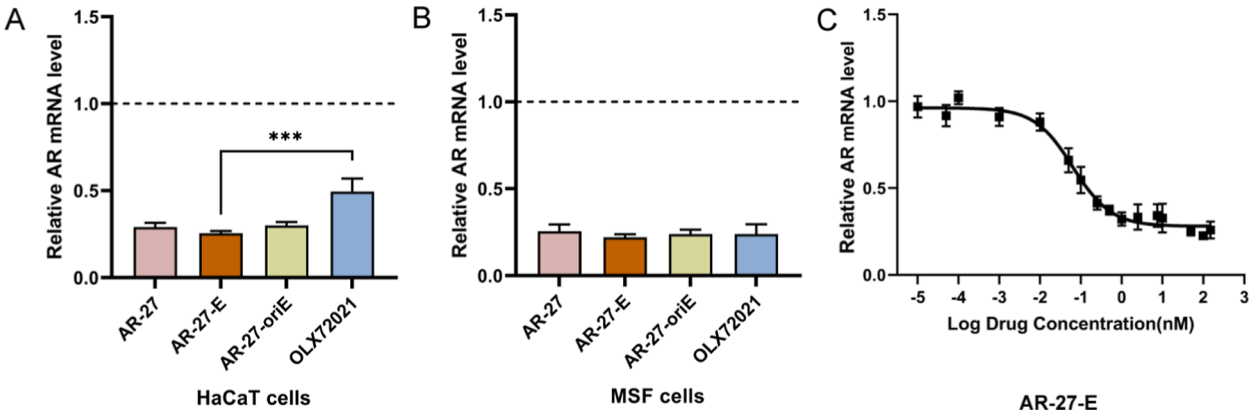

Figure 1. Efficacy of AR-27 and its derivative sequences with chemical modification in vitro. (A) Efficacy of AR mRNA level in HaCaT cells. (B) Efficacy of AR mRNA level in MSF cells. (C) IC_{50} of AR-27 E in HaCaT cells. AR-27 E was AR-27 with chemical modification and TT overhanging base terminus. AR-27-OriE was AR-27 E with mRNA pairing base terminus instead of TT overhanging base terminus. Data were shown as mean ± SEM ($n \geq 3$). p values were calculated with the one-way analysis of variance (ANOVA) test. *$p < 0.05$, **$p < 0.01$, ***$p < 0.001$, and ****$p < 0.0001$.

provide new direction for disease treatment and six siRNA drugs have already been approved by FDA up to 2025.[24−29] OLX72021,[30] a siRNA targeting CDS region of AR transcript, was developed for AGA and its Phase I clinical trial was completed in Australia in January 2025.[31] Chemical modifications and delivery systems have not only bolstered the stability and delivery efficacy of siRNAs[32] but also extended the duration of RNA interference, lengthened their half-life, enhanced metabolic kinetics, and enabled long-term therapeutic effects.[33,34] These advancements collectively position siRNAs as highly promising candidates for the treatment of chronic diseases.

Studies have shown that siRNA targeting within the untranslated region (UTR) performed as effective as targeting within the CDS[35] and had elevated mismatch tolerance due to translational repression in addition to mRNA degradation.[36] In addition, off-target effects of siRNA could be partly avoided by targeting conserved sequences within the UTR of transcripts.[37] Targeting CFLm25 to reprogram the 3′ UTR of tumor suppressor genes could achieve alternative polyadenylation (APA)-based post-transcriptional regulation and further GBM therapy.[38] A siRNA designed for the 3′UTR region of Zika virus (ZIKV) was able to significantly inhibit ZIKV replication, which was considered as a potential therapeutic.[39] Different from OLX72021, we designed a series of AR-targeting siRNAs based on the UTR region of full length AR transcript for AR gene silencing. Among these siRNAs, a homeotic siRNA sequence for*Homo sapiens*and*Mus musculus*((designated AR-27 E) was identifed through siRNA screening in HaCaT cells and was equally effective in mouse skin fibroblasts (MSF cells). The cholesterol-conjugate of AR-27 E (AR-27 E-Chol) was further used for in vivo treatment of AGA in AGA-like model mice. The dorsal hair growth and follicle proliferation as well as molecular levels of AR mRNA and protein in AGA-like model mice were investigated with the treatment of AR-27 E-Chol.

RESULTS

Design and Screening of siRNAs Targeting the UTR Region of AR Gene. Different from OLX72021 targeting the CDS region of AR gene, all AR siRNAs listed in Table S1 were designed to target the UTR region of AR gene (NM_000044.6) and their gene silencing capabilities were screened in HaCaT cells to evaluate their potential in downregulating AR gene expression. As shown in Figure S1 and Table S1, AR mRNA was downregulated to 47.6 ± 2.0% by OLX72021 and other 13 AR siRNAs such as AR-5, AR-6, AR-9, AR-23, AR-27, AR-30, AR-33, AR-34, AR-41, AR-44, AR-50, AR-52, and AR-58 demonstrated better gene knockdown efficacy. Among them, AR-27 exhibited the highest gene knockdown efficacy with silencing of the AR mRNA to 29.1 ± 2.4%. Subsequently, the aforementioned AR siRNA sequences were individually subjected to chemical modifications including phosphorothioate backbone, 2′-*O*-methyl (2′-OMe), 2′-fluoro (2′-F), and terminal cholesterol conjugation and the gene knockdown effects of these modified siRNAs were further evaluated (Table S2). In combination with AR gene transcripts in different species, AR-27, AR-30, AR-33, AR-34, and AR-41 siRNA sequences exhibited high homology in human and mouse (Table S3) and all of these siRNAs could also effectively knockdown the mouse AR mRNA in MSF cells (Figure S3). Based on above-mentioned screening results, AR-27 was selected for subsequent experiments due to its superior performance in AR gene silencing.

As shown in Figure 1A, AR mRNA was downregulated to 25.5 ± 1.3% in HaCaT cells by AR-27 E with chemical modifications of nucleotides, which was slightly better than AR-27 (29.1 ± 2.4%) and AR-27-oriE (29.9 ± 1.9%) but 1.8-fold higher than OLX72021 (47.6 ± 2.0%), indicating that AR-27 was a preferred siRNA sequence for AR gene silencing and its chemical modification of sequences did not have an obvious negative effect on the silencing efficacy of AR gene. In MSF cells, AR mRNA was silenced to 21.9 ± 1.7% by AR-27 E, which also had no obvious difference with AR-27 (25.4 ± 3.9%) and AR-27-OriE (23.8 ± 2.6%) (Figure 1B). In comparison to OLX72021 (23.9 ± 3.9%), AR-27 E showed a similar AR gene knockdown in mouse MSF cells (Figures 1B and S2) but displayed more efficient gene silencing activity in human HaCaT cells (Figure 1A). IC_{50} values for all of the modified siRNAs were also investigated as shown in Figures 1C and S3, and AR-27 E had the lowest IC_{50} value of 0.064 nM under the same experimental conditions. These findings indicated that AR-27E achieved the most effective AR gene silencing in both HaCaT and MSF cells and displayed a better efficacy than OLX72021 in human HaCaT cells.

https://doi.org/10.1021/acs.jmedchem.5c01739
J. Med. Chem. 2025, 68, 20586−20594

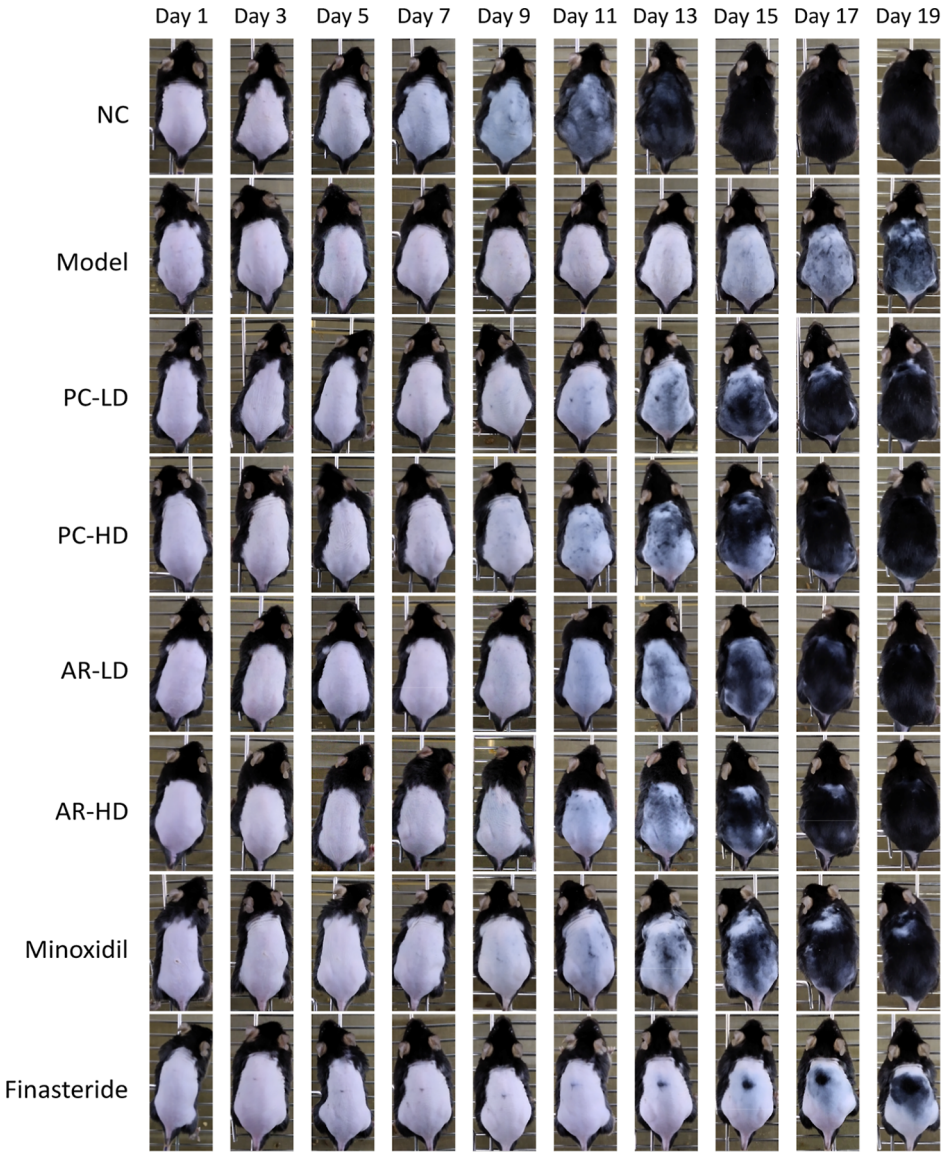

Figure 2. Dorsal hair growth in mice with various treatments for 19 days including normal mice (NC), androgenetic alopecia mice intradermally injected with PBS (Model), OLX72021 (5 mg/kg for PC-LD and 25 mg/kg for PC-HD), AR-27 E-Chol (5 mg/kg for AR-LD and 25 mg/kg for AR-HD), and androgenetic alopecia mice tropically treated with 2.2% minoxidil gel (Minoxidil) and orally treated with finasteride (Finasteride).

AR Gene Silencing in the Androgenetic Alopecia Mouse Model by AR-27 E-Chol. AR gene silencing in vivo and AGA treatment were investigated using cholesterol-conjugated AR-27 E (AR-27 E-Chol) through intradermic delivery. AGA-like model mice were mimicked through intraperitoneal administration of dihydrotestosterone (DHT) daily. Two doses at 5 and 25 mg/kg of both AR-27 E-Chol (AR-LD, AR-HD) and positive control OLX72021 (PC-LD and PC-HD) were intradermally injected to the mice's dorsal skin. Minoxidil gel was applied topically, and finasteride was administered orally as additional positive controls. As shown in Figures 2 and S5, AGA-like model mice exhibited pink dorsal skin with significantly slower dorsal hair growth in the anagen of mice from day 7 to day 9 compared to the NC group, while the dorsal hair of AGA-like model mice rarely covered the dorsal skin even at the end of treatment. Based on the skin color assessment scale (Figure 3A), the color of dorsal skin transitioned to gray and dorsal hair grew in PC-LD, PC-HD, AR-LD, AR-HD, and minoxidil groups from day 13, whereas AGA-like model mice still maintained bare pink skin. With the natural progression of mice hair growth cycle, the dorsal skin color of PC-LD, PC-HD, AR-LD, AR-HD, and minoxidil groups had no significant visual difference in comparison to the NC group at the end of treatment, whereas AGA-like model mice and finasteride group exhibited obviously decreased hair density (Figure 3C). On the end of the treatment at day 19, the dorsal hair of PC-LD, PC-HD, AR-LD, AR-HD, and minoxidil groups almost fully covered dorsal skin, while the dorsal hair of the AGA-like model and finasteride groups remained sparse with lengths of 3.1 ± 0.1 and 3.3 ± 0.4 mm, respectively (Figure 3B). Instead, the dorsal hair of the AR-27 E-Chol group grew to 4.1 ± 0.1 mm (AR-LD) and 4.6 ± 0.1 mm (AR-HD), which was significantly higher than AGA-like model and finasteride groups but had no obvious difference with the OLX72021 group (4.4 ± 0.1 mm for PC-LD and 4.4 ± 0.1 mm for PC-HD) and minoxidil group (4.4 ± 0.1 mm). These results clearly demonstrated that AR siRNA obviously alleviated the AGA-like symptoms in AGA-like model mice,

https://doi.org/10.1021/acs.jmedchem.5c01739
J. Med. Chem. 2025, 68, 20586−20594

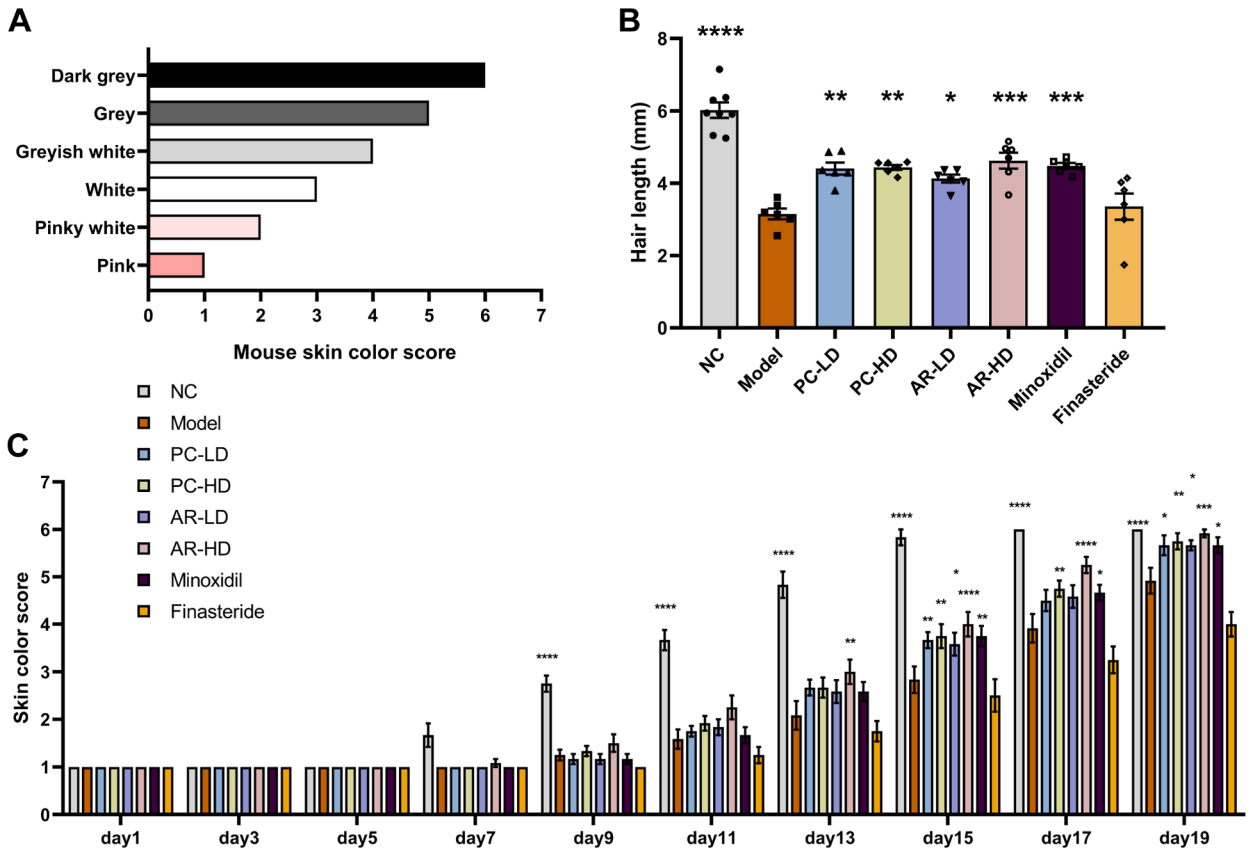

Figure 3. Physical efficacies of different treatments in AGA-like model mice. (A) Mouse skin color score criteria. (B) Length of growth dorsal hair at the end of treatment. (C) Skin color scores of mice based on the mouse skin color score criteria. The mice included normal mice (NC), androgenetic alopecia mice with PBS (Model), androgenetic alopecia mice with OLX72021 in 5 mg/kg (PC-LD), androgenetic alopecia mice with OLX72021 in 25 mg/kg (PC-HD), androgenetic alopecia mice with AR-27 E-Chol in 5 mg/kg (AR-LD), androgenetic alopecia mice with AR-27 E-Chol in 25 mg/kg (AR-HD), androgenetic alopecia mice with 2.2% minoxidil gel (Minoxidil), and androgenetic alopecia mice with oral finasteride (Finasteride). Data are shown as mean ± SEM ($n = 6$). p values were calculated with the one-way ANOVA test. *$p < 0.05$, **$p < 0.01$, ***$p < 0.001$, and ****$p < 0.0001$.

with dorsal hair growth comparable to minoxidil and OLX72021 while outperforming finasteride.

As shown in Figure 4A, distinct hair follicle cycling phases were observed across the treatment groups. Dark purple-stained hair follicles located at the deep dermis exhibited characteristic anagen morphology, while light purple-stained follicles at the superficial dermis displayed typical telogen features. The hair follicles of AGA-like model mice remained in the telogen phase, and the diameter was shorter than the inner root sheath, which was a typical pathological change of AGA. In contrast, both AR-LD and AR-HD treatment groups exhibited numerous anagen-phase follicles, showing morphological and structural characteristics comparable to those in the NC group, PC-LD, PC-HD, and minoxidil-treated mice. Notably, finasteride-treated mice showed sparse hair growth with slightly enlarged follicles transitioning to the catagen phase. The anagen-to-telogen (A/T) ratio, a key indicator of follicular growth capacity, was systematically quantified (Figure 4B). All treatments enhanced the A/T ratio, which was significantly higher than the AGA-like mice model (0.5 ± 0.3), and AR-HD induced the highest A/T ratio to 3.9 ± 0.3 among them. As previously reported in the literature, OLX72021 could also induce hair follicle growth,[30] which increased A/T ratio to 3.2 ± 0.6 for PC-LD and 3.2 ± 0.5 for PC-HD, respectively. In comparison to OLX72021, AR siRNA significantly induced higher growth capacity on AGA-like model mice with A/T ratios of 3.7 ± 0.4 for AR-LD and 3.9 ± 0.3 for AR-HD, which showed a slightly superior effect compared to OLX72021, especially at high dose. In addition, the A/T ratios of Minoxidil and Finasteride were 2.8 ± 0.4 and 3.3 ± 0.4, which were lower than those of AR-LD and AR-HD. The above findings demonstrated that AR siRNA successfully promoted dorsal hair follicle recovery in AGA-like mice.

Molecular analysis of AR expression was also performed for all the mice skin tissue samples. The AR transcriptional level in AGA-like model mice was 1.3-fold higher than that in normal mice. However, all treatment groups showed significant AR mRNA suppression of 45.1 ± 5.2% in AR-LD; 61.5 ± 5.8% in AR-HD; 64.7 ± 8.4% in PC-LD; 67.3 ± 9.2% in PC-HD; 61.7 ± 6.2% in minoxidil; and 64.5 ± 4.9% in finasteride (Figure 4C). As shown in Figure 4D,E, the AR protein level of AGA-like model mice was 2.1-fold higher than that of normal mice. Minoxidil and finasteride treatment slightly downregulated the AR protein levels versus AGA-like model mice but still maintained higher AR protein levels than the NC group (1.6-fold and 1.8-fold, respectively). After 5 mg/kg of OLX72021 treatment (PC-LD), the AR protein level was downregulated to 66.7% compared with AGA-like model mice, yet still remaining a little bit higher than normal mice (1.4-fold). Increasing OLX72021 concentration to 25 mg/kg (PC-HD), significant AR protein downregulation was observed (21.1 ± 5.3%). The AR protein level of AR-27 E-Chol at 5 mg/kg (AR-

https://doi.org/10.1021/acs.jmedchem.5c01739
J. Med. Chem. 2025, 68, 20586−20594

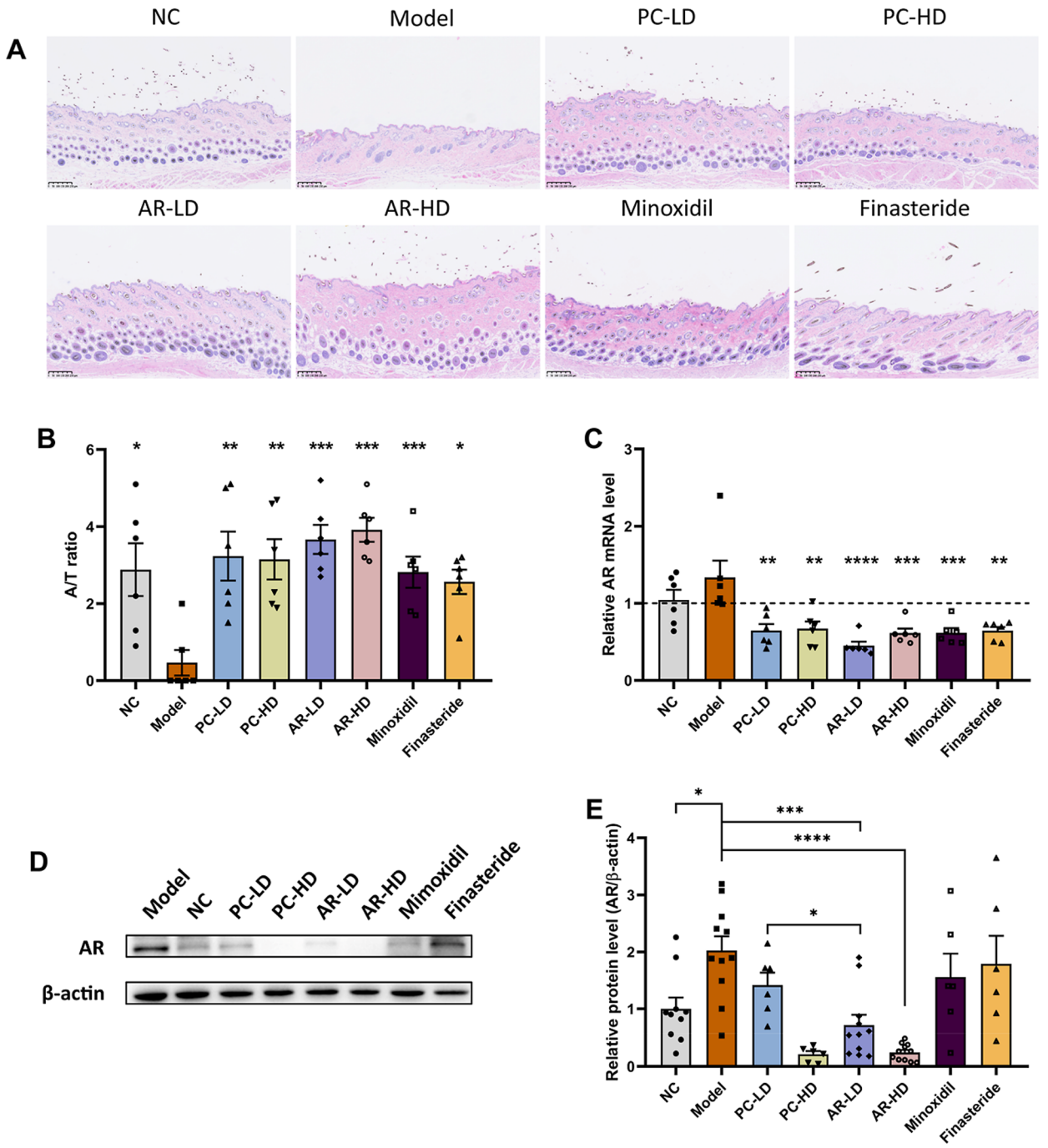

Figure 4. Hair follicle proliferation and AR gene expression under different treatment groups. (A) H&E staining images of dorsal skin. Scale bar = 250 μm. (B) A/T ratios in mice quantified from H&E staining images (A/T ratio = anagen hair follicles/telogen hair follicles). (C) AR mRNA level in dorsal skin of drug treatment site. (D) Representative Western blotting image of AR protein expression. (E) Quantification of AR and β-actin protein level in dorsal skin of the drug treatment site. The mice included normal mice (NC), androgenetic alopecia mice with PBS (Model), androgenetic alopecia mice with OLX72021 in 5 mg/kg (PC-LD), androgenetic alopecia mice with OLX72021 in 25 mg/kg (PC-HD), androgenetic alopecia mice with AR-27 E-Chol in 5 mg/kg (AR-LD), androgenetic alopecia mice with AR-27 E-Chol in 25 mg/kg (AR-HD), androgenetic alopecia mice with 2.2% minoxidil gel (Minoxidil), and androgenetic alopecia mice with oral finasteride (Finasteride). Data were shown as mean ± SEM (n = 6). p values were calculated with the one-way ANOVA test. *p < 0.05, **p < 0.01, ***p < 0.001, and ****p < 0.0001.

LD) was knockdown to 35.4% compared with AGA-like model mice, which was about 2-fold more efficient downregulation than that of PC-LD. At 25 mg/kg of AR-27 E-Chol (AR-HD), the AR protein level was further decreased with about 8.4-fold downregulation versus AGA-like model mice and 4.1-fold downregulation versus normal mice (24.1 ± 4.4%). Thus, AR-27 E-Chol demonstrated superior efficacy to OLX72021 at the low dose of 5 mg/kg based on AR protein expression. However, the advantage diminished with the increase of siRNA dose to 25 mg/kg.

To further validate the therapeutic effects of AR-27 E-Chol on AGA-like hair follicle growth, the expression of the proliferation marker Ki67 was verified in skin tissue sections by immunohistochemical analysis. As shown in Figure 5, the

https://doi.org/10.1021/acs.jmedchem.5c01739
J. Med. Chem. 2025, 68, 20586−20594

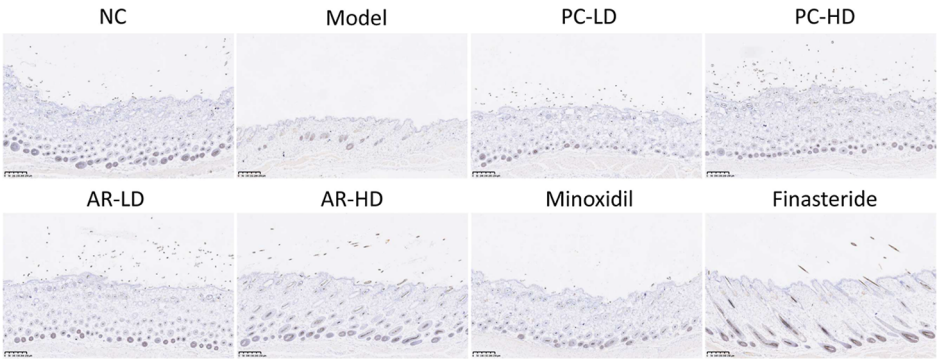

Figure 5. Hair follicles proliferation at the end of treatment evaluated by immunohistochemistry staining images of the proliferation marker Ki67. Scale bar = 250 μm. The mice included normal mice (NC), androgenetic alopecia mice with PBS (Model), androgenetic alopecia mice with OLX72021 in 5 mg/kg (PC-LD), androgenetic alopecia mice with OLX72021 in 25 mg/kg (PC-HD), androgenetic alopecia mice with AR-27 E-Chol in 5 mg/kg (AR-LD), androgenetic alopecia mice with AR-27 E-Chol in 25 mg/kg (AR-HD), androgenetic alopecia mice with 2.2% minoxidil gel (Minoxidil), and androgenetic alopecia mice with oral finasteride (Finasteride).

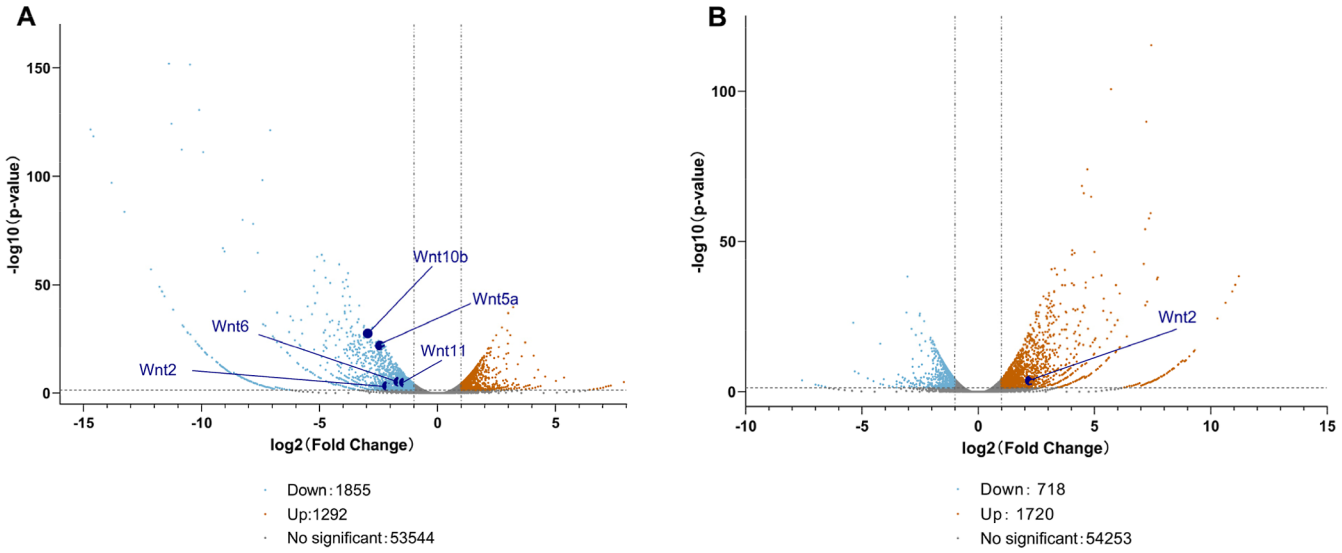

Figure 6. Transcriptomic analysis of mouse skin tissue samples in the model mice group and AR-27 E-Chol treatment. (A) Volcano plot summarizing the up- and downregulated genes after AGA modeling. (B) Volcano plot summarizing the up- and downregulated genes after AR-27 E-Chol treatment.

NC group exhibited abundant Ki67$^+$ cells in the dermis, indicating the active hair follicle growth. In contrast, AGA-like model mice exhibited significantly fewer Ki67$^+$ cells, consistent with the telogen-phase arrest of most hair follicle cells at the end of the experiment. Compared to AGA-like model mice, all treated groups (PC-LD, PC-HD, AR-LD, AR-HD, minoxidil group, and finasteride group) demonstrated a marked increase in Ki67$^+$ cells, suggesting their promotion of hair follicle proliferation and alleviation of the AGA symptoms. Among these treated groups, the groups with siRNA treatment (PC-LD, PC-HD, AR-LD, AR-HD) showed denser Ki67$^+$ cells than the small molecule-treated groups, especially the finasteride group. In addition to therapeutical efficacy, the safety and systemic toxicity were also assessed. The body weights of mice in all the groups slightly increased during the treatment, with no obvious differences (Figure S4A). The main organs of mice including heart, liver, spleen, lung, and kidney were also isolated and weighed with all falling within normal physiological ranges (Figure S4B). H&E staining images of organs also showed normal morphology, indicating the safety of AR-27 E-Chol treatment (Figure S4C). In addition, the representative biomarkers of liver and kidney functions were evaluated, and the levels of ALT, BUN, and CREA in C57BL/6J mice serum were all within the normal reference range (Figure S13). All of these data confirmed that AR-27 E-Chol is a safe siRNA drug candidate with low system toxicity for androgenic alopecia treatment.

Collaborative Regulatory Effect of AR siRNA via the Wnt/β-Catenin Pathway in the AGA-like Mouse Model. Given the interaction between AR and Wnt/β-catenin signaling pathways in AGA pathogenesis,[40] we performed transcriptomic analysis of mouse skin tissue samples following AR-27 E-Chol treatment. As shown in Figure 6A, up to 1855 genes were downregulated in AGA-like model mice. Among these, several Wnt family genes, including Wnt10b, Wnt5a, Wnt6, Wnt11, and Wnt2, were significantly downregulated, indicating suppression of Wnt signaling upon AGA induction. Upon treatment of AR-27 E-chol in AGA-like mice (Figure 6B), 1720 genes were upregulated compared to normal mice. Notably, Wnt2 was significantly elevated beyond normal levels, while other Wnt family members were restored to the normal level. These results suggested that AR-27 E-Chol-induced AR

https://doi.org/10.1021/acs.jmedchem.5c01739
J. Med. Chem. 2025, 68, 20586−20594

silencing (Figure 4D) alleviated the interaction between AR and β-catenin, thereby reactivating the Wnt pathway. To further validate the crosstalk between Wnt/β-catenin and AR signaling, we performed immunohistochemical (IHC) staining for Wnt5a (Figure S16) and β-catenin (Figure S17). As shown in Figures S16 and S17, in AGA-like mice, both Wnt5a and β-catenin were nearly absent in hair follicles, consistent with efficient suppression of Wnt signaling under high AR activity. In contrast, all treatment groups, especially those receiving RNAi-mediated AR silencing, showed clear recovery of Wnt5a and β-catenin expression. Moreover, hair follicles in the AR-LD and AR-HD groups exhibited more dense and intense IHC signals for Wnt5a compared to those treated with OLX72021 or Minoxidil. All these findings confirmed that AR-27 E-Chol effectively silenced AR gene expression, leading to coordinated reactivation of the Wnt/β-catenin pathway and promotion of hair follicle proliferation, underscoring its potential as a therapeutic strategy for AGA.

CONCLUSIONS

Targeting the UTR region of transcripts has been proven to be an effective strategy for designing siRNA therapeutics. A notable example is Inclisiran, the FDA-approved siRNA therapeutic (2021), which targets the non-coding region of PCSK9 mRNA.[41] In this study, we developed a series of AR-targeting siRNAs based on the UTR region of AR transcripts. Among these siRNAs, AR-27 E could target the homologous AR transcript sequence of *H. sapiens* and*M. musculus* and exhibited the outstanding AR gene silencing efficacy in both human HaCaT cells and mouse MSF cells, significantly reducing the AR mRNA expression in HaCaT cells (IC_{50} = 0.064 nM). Intradermal administration of the cholesterol conjugate of AR-27 E (AR-27 E-Chol) significantly alleviated AGA symptoms, as evidenced by the dorsal hair growth, dorsal hair follicles proliferation, and significant downregulation of AR mRNA and protein expression in skin tissues of AGA-like mice. In addition, AR-27 E-Chol treatment collaboratively reversed the inhibition of the Wnt/β-catenin pathway, as evidenced by the transcriptional expression enhancement of the Wnt family and positive expression of Wnt5a and β-catenin in IHC. Thus, AR-27 E-Chol demonstrated therapeutic efficacy comparable to the FDA-approved drug minoxidil, with a synergistic impact on both AR signaling downregulation and Wnt/β-catenin pathway activation, suggesting that AR-27 E-Chol holds the potential as a safe and effective treatment for androgenetic alopecia.

METHOD

Oligonucleotides. All siRNAs in Table S1 were purchased from Primerna Biotechnology (Shanghai, China) with ≥95% purity by HPLC analysis. All primers in Table S4 were purchased from Sangon Biotech (Shanghai, China).

MATERIALS

PBS, trypsin (0.25%), Dulbecco's Modified Eagle Medium (DMEM) complete medium, Penicillin−Streptomycin (100×) were purchased from M&C (China). Opti-MEM was purchased from Gibco. Fetal Bovine Serum (FBS) was purchased from Procell (China). Lipofectamine 2000 transfection reagent was purchased from Thermo Fisher. Dihydrotestosterone (DHT) was purchased from Solarbio (China). Finasteride was purchased from Yuanye (Shanghai, China).

Cell Lines and Animals. HaCaT cells were provided by the Peking University First Hospital. MSF cells were purchased from Procell (China). All C57BL/6J mice used in this study were purchased and maintained from the Department of Laboratory Animal Science of Peking University Health Science Center. The procedures of animal experiments were approved by the Institutional Animal Care and Use Committee of Peking University Health Science Center.

Cell Culture and Transfection. HaCaT cells and MSF cells were cultured in DMEM medium containing 10% FBS and 1% penicillin−streptomycin (DMEM complete medium) at 37 °C for a humidified atmosphere with 5% CO_2. The cells were transfected with the lipofectamine 2000/siRNA complex. Lipofectamine 2000 was added into Opti-MEM for 5 min incubation and then added into siRNA Opti-MEM solution for another 15 min incubation at room temperature to form the lipofectamine 2000/siRNA complex.

RT-qPCR. HaCaT cells were seeded into 24-well plates with 500 μL of cell suspension of 5×10^4 cells per well and incubated for 24 h. The cells were transfected with the lipofectamine 2000/siRNA complex at the final siRNA concentration of 50 nM. After transfection for 6 h, the mediums were replaced by fresh DMEM complete medium for another 42 h of incubation. Total RNA was extracted with the Trizol Reagent (vazyme, China) and reversely transcribed to cDNA using Uni All-in-One First-Strand cDNA Synthesis SuperMix for qPCR Kit (TransGen, China) according to protocols. The cDNA was quantified by the qRT-PCR system with qPCR SuperMix (TransGen, China) according to protocols. GAPDH (glyceraldehyde 3-phosphate dehydrogenase) gene was used as the internal control. Primers were listed as follows: AR (human), forward: 5′-CAT TTT GCA TGC GCT CTG CT-3′ and reverse: 5′-GCT CAC CAG CTA AGT GGG TC-3′; GAPDH, forward: 5′-TGC ACC AAC TGC TTA GC-3′ and reverse: 5′-GGC ATG GAC TGT GGT CAT GAG-3′.

For qRT-PCR of the mice AR gene, the dorsal skin tissues were cut into pieces and crushed in the Trizol reagent. Total RNA was reversely transcribed to cDNA and further quantified by the qRT-PCR system. RPL32 gene was used as the internal control. Primers were listed as follows: AR (mouse), forward: 5′-AGC CCA TCT ATT TCC ACA CAC-3′ and reverse: 5′-GAG GAA TTT CCC CCA AGG CA-3′; RPL32, forward: 5′- CTG CCA TCT GTT TTA CGG CA-3′ and reverse: 5′-ATC AGG ATC TGG CCC TTG AAC-3′

Western Blot. For the Western blot of mice AR protein, the dorsal skin tissues were cut into pieces and crushed in RIPA Lysis buffer (Macgene, China) with protease inhibitor and phosphatase inhibitor. The concentration of total protein was determined with a BCA protein assay kit (Beyotime, China). Samples were loaded on SDS-PAGE gel and transferred to a nitrocellulose membrane (Millipore) for blotting. The membranes were blocked with 5% nonfat milk for 1 h at room temperature and then incubated with AR primary antibody (ab133273, Abcam) at 4 °C overnight. After washing with 1 × TBST buffer three times, the membranes were incubated with a secondary antibody (ZB-2301, ZSGB-Bio) for 1 h at room temperature. Further washing the membranes with 1 × TBST buffer three times, the signals of AR protein (110 kDa) was detected by the Western Blot Imaging System (Tanon 5200) using an enhanced chemiluminescent detection reagent kit (Biodragon, China). After stripping, the membranes were incubated with β-actin primary antibody (LF202, Epizyme) at 4 °C overnight. The membranes were washed with 1 × TBST buffer three times, incubated with a second antibody, and exposed for detecting β-actin (43 kDa) signal.

AR siRNA Efficacy In Vivo. All animal experiments were approved by the Committee for Animal Research of Peking University (permission NO: DLASBD0267). Male C57BL/6J mice (8 weeks, Department of Laboratory Animal Science, Peking University Health Science, Beijing, China) were maintained for 1 week of adaptation, followed by intraperitoneal administration with DHT (1 mg/day, dissolved in corn oil) for AGA-like model mice or only corn oil for the control group. After four-day DHT administration, the mice were depilated with depilatory cream to remove dorsal hair and randomly divided into 8 groups (6 mice for each group) including control group (NC), AGA-like model mice group (Model), and model mice with the treatment of 5 mg/kg OLX72021 (PC-LD), 25 mg/kg OLX72021 (PC-HD), 5 mg/kg AR-27 E-Chol (AR-LD), 25 mg/kg AR-27 E-

https://doi.org/10.1021/acs.jmedchem.5c01739
J. Med. Chem. 2025, 68, 20586−20594

Chol (AR-HD), daily 2.2% minoxidil gel group (Minoxidil), and oral 10mg/kg finasteride group (Finasteride). All the mice with siRNA treatment were injected intradermally every 4 days. AR-27 E-Chol was injected at the upper right sites on the mice dorsal skin, and every injection volume was under 50 μL. For distinct medication days, the injection sites were apart from each other to avoid local reactions. The body weights of mice were recorded, and the photographs of dorsal hair growth were taken every 2 days. All the mice were anesthetized with isoflurane and sacrificed on the 19th day after depilation. Dorsal skin tissues were collected for histopathology and biochemical assays.

Statistical Analyses. The statistical variations between the control group and the treatment groups were determined by the one-way ANOVA test. The data were presented as mean ± SEM, and p values were presented for $p < 0.05$ ($^{*}p < 0.05$, $^{**}p < 0.01$, $^{***}p < 0.001$, and $^{****}p < 0.0001$).

■ ASSOCIATED CONTENT

Supporting Information

The Supporting Information is available free of charge at https://pubs.acs.org/doi/10.1021/acs.jmedchem.5c01739.

SiRNA sequences; HPLC trace; homology analysis of AR siRNA; IC_{50} values; and additional experimental details in vitro and in vivo (PDF)

■ AUTHOR INFORMATION

Corresponding Authors

Jing Wang − *State Key Laboratory of Natural and Biomimetic Drugs, Chemical Biology Center and School of Pharmaceutical Sciences, Peking University, Beijing 100191, China; Peking University Ningbo Institute of Marine Medicines, Ningbo 315832, China;* orcid.org/0000-0001-8369-7453; Email: wangjing1988@bjmu.edu.cn

Xinjing Tang − *State Key Laboratory of Natural and Biomimetic Drugs, Chemical Biology Center and School of Pharmaceutical Sciences, Peking University, Beijing 100191, China; Peking University Ningbo Institute of Marine Medicines, Ningbo 315832, China;* orcid.org/0000-0002-9959-1167; Email: xinjingt@hsc.pku.edu.cn

Authors

Di Feng − *State Key Laboratory of Natural and Biomimetic Drugs, Chemical Biology Center and School of Pharmaceutical Sciences, Peking University, Beijing 100191, China*

Xinli Fan − *Medical and Health Analysis Center, Peking University, Beijing 100191, China*

Yuqiang Hu − *State Key Laboratory of Natural and Biomimetic Drugs, Chemical Biology Center and School of Pharmaceutical Sciences, Peking University, Beijing 100191, China*

Yizhi Man − *State Key Laboratory of Natural and Biomimetic Drugs, Chemical Biology Center and School of Pharmaceutical Sciences, Peking University, Beijing 100191, China*

Qian Wang − *State Key Laboratory of Natural and Biomimetic Drugs, Chemical Biology Center and School of Pharmaceutical Sciences, Peking University, Beijing 100191, China; Peking University Ningbo Institute of Marine Medicines, Ningbo 315832, China*

Yanmin Song − *Cosychem Technology (Tianjin) Co., Ltd., Tianjin 300450, China*

Jingjing Zhou − *Cosychem Technology (Tianjin) Co., Ltd., Tianjin 300450, China*

Jin Zhang − *Cosychem Technology (Tianjin) Co., Ltd., Tianjin 300450, China*

Yun Luo − *Shanghai Primerna Biotechnology Co. Ltd, Shanghai 201600, China*

Complete contact information is available at: https://pubs.acs.org/10.1021/acs.jmedchem.5c01739

Author Contributions

[#]D.F., X.F., and Y.H. contributed equally to this work. D.F.: performed in vitro and in vivo experiments and wrote the initial draft of the manuscript. X.F.: performed in vivo experiments, data analysis, and manuscript writing. Y.H.: assisted in vivo experiments. Y.M.: assisted in vivo experiments. Q.W.: assisted in vitro experiments and manuscript writing. Y.S.: directed the project. J.J.Z.: directed the project and manuscript discussion. J.Z.: performed RT-qPCR experiments and data analysis. Y.L.: synthesized siRNA sequences and characterization. J.W.: directed the project, assisted in vitro experiment data analysis, and manuscript writing. X.T.: designed and directed the project as well as performed data analysis and manuscript writing. The manuscript was written through contributions of all authors. All authors have given approval to the final version of the manuscript.

Notes

The authors declare no competing financial interest.

■ ACKNOWLEDGMENTS

This work was supported by the PKU Health Science Center & Cosychem Joint Laboratory of Nucleic Acid Drug Innovation Research (L202304) and the National Natural Science Foundation of China (Grant Nos. 22277003 and 22207006).

■ ABBREVIATIONS

AGA, androgenetic alopecia; AR, androgen receptor; CDS, coding sequence; DHT, dihydrotestosterone; DP, dermal papilla cells; HaCaT, human immortalized keratinocyte cell line; MSF, mouse skin fibroblasts; siRNA, small-interfering RNA; UTR, untranslated region

■ REFERENCES

(1) Bansod, S.; Sharma, A.; Mhatre, M. Androgenetic Alopecia: Clinical Features and Trichoscopy. *Clin. Dermatol. Rev.* **2022**, *6* (2), 63.

(2) Lee, W.-S.; Ro, B. I.; Hong, S. P.; Bak, H.; Sim, W.-Y.; Kim, D. W.; Park, J. K.; Ihm, C.-W.; Eun, H. C.; Kwon, O. S.; Choi, G. S.; Kye, Y. C.; Yoon, T. Y.; Kim, S.-J.; Kim, H. O.; Kang, H.; Goo, J.; Ahn, S.-Y.; Kim, M.; Jeon, S. Y.; Oh, T. H. A New Classification of Pattern Hair Loss That Is Universal for Men and Women: Basic and Specific (BASP) Classification. *J. Am. Acad. Dermatol.* **2007**, *57* (1), 37−46.

(3) Kim, B. J.; Choi, J.; Choe, S. J.; Lee, S.; Lee, W.-S. Modified Basic and Specific (BASP) Classification for Pattern Hair Loss. *Int. J. Dermatol.* **2020**, *59* (1), 60−65.

(4) Gentile, P.; Garcovich, S. Advances in Regenerative Stem Cell Therapy in Androgenic Alopecia and Hair Loss: Wnt Pathway, Growth-Factor, and Mesenchymal Stem Cell Signaling Impact Analysis on Cell Growth and Hair Follicle Development. *Cells* **2019**, *8* (5), 466.

(5) Otberg, N.; Finner, A. M.; Shapiro, J. Androgenetic Alopecia. *Endocrinol. Metab. Clin. North Am.* **2007**, *36* (2), 379−398.

(6) Urysiak-Czubatka, I.; Kmieć, M. L.; Broniarczyk-Dyła, G. Assessment of the Usefulness of Dihydrotestosterone in the Diagnostics of Patients with Androgenetic Alopecia. *Adv. Dermatol. Allergol.* **2014**, *31* (4), 207−215.

(7) Tsuboi, R.; Niiyama, S.; Irisawa, R.; Harada, K.; Nakazawa, Y.; Kishimoto, J. Autologous Cell−Based Therapy for Male and Female Pattern Hair Loss Using Dermal Sheath Cup Cells: A Randomized Placebo-Controlled Double-Blinded Dose-Finding Clinical Study. *J. Am. Acad. Dermatol.* **2020**, *83* (1), 109−116.
(8) Ellis, J. A.; Sinclair, R.; Harrap, S. B. Androgenetic Alopecia: Pathogenesis and Potential for Therapy. *Expert Rev. Mol. Med.* **2002**, *4* (22), 1−11.
(9) Ellis, J. A.; Stebbing, M.; Harrap, S. B. Polymorphism of the Androgen Receptor Gene Is Associated with Male Pattern Baldness. *J. Invest. Dermatol.* **2001**, *116* (3), 452−455.
(10) Orasan, M. S.; Roman, I. I.; Coneac, A.; Muresan, A.; Orasan, R. I. Hair Loss and Regeneration Performed on Animal Models. *Med. Pharm. Rep.* **2016**, *89* (3), 327−334.
(11) Olsen, E. A.; Whiting, D.; Bergfeld, W.; Miller, J.; Hordinsky, M.; Wanser, R.; Zhang, P.; Kohut, B. A Multicenter, Randomized, Placebo-Controlled, Double-Blind Clinical Trial of a Novel Formulation of 5% Minoxidil Topical Foam versus Placebo in the Treatment of Androgenetic Alopecia in Men. *J. Am. Acad. Dermatol.* **2007**, *57* (5), 767−774.
(12) Andy, G.; John, M.; Mirna, S.; Rachita, D.; Michael, K.; Maja, K.; Aseem, S.; Zeljana, B. Controversies in the Treatment of Androgenetic Alopecia: The History of Finasteride. *Dermatol. Ther.* **2019**, *32* (2), No. e12647.
(13) Overstreet, J. W.; Fuh, V. L.; Gould, J.; Howards, S. S.; Lieber, M. M.; Hellstrom, W.; Shapiro, S.; Carroll, P.; Corfman, R. S.; Petrou, S.; Lewis, R.; Toth, P.; Shown, T.; Roy, J.; Jarow, J. P.; Bonilla, J.; Jacobsen, C. A.; Wang, D. Z.; Kaufman, K. D. Chronic Treatment with Finasteride Daily Does Not Affect Spermatogenesis or Semen Production in Young Men. *J. Urol.* **1999**, *162* (4), 1295−1300.
(14) May, E.; Jodl, S. J.; KräTzschmar, J.; Otto, C. Prolactin Receptor Antibody for Male and Female Pattern Hair Loss. US20210128728A1, May 6, 2021. https://patents.google.com/patent/US20210128728A1/en (accessed 2025−07−23).
(15) Sheppard, M.; Laskou, F.; Stapleton, P. P.; Hadavi, S.; Dasgupta, B. Tocilizumab (Actemra). *Hum. Vaccines Immunother.* **2017**, *13* (9), 1972−1988.
(16) Zheng, M.; Kim, M.-H.; Park, S.-G.; Kim, W.-S.; Oh, S.-H.; Sung, J.-H. CXCL12 Neutralizing Antibody Promotes Hair Growth in Androgenic Alopecia and Alopecia Areata. *Int. J. Mol. Sci.* **2024**, *25* (3), 1705.
(17) Choi, N.; Hwang, J.; Kim, D. Y.; Kim, J.; Song, S. Y.; Sung, J.-H. Involvement of DKK1 Secreted from Adipose-Derived Stem Cells in Alopecia Areata. *Cell Proliferation* **2024**, *57* (3), No. e13562.
(18) Jin, S.-E.; Kim, J.; Sung, J.-H. Recent Approaches of Antibody Therapeutics in Androgenetic Alopecia. *Front. Pharmacol* **2024**, *15*, 1434961.
(19) Xu, Z.; Leu, J. H.; Xu, Y.; Nnane, I.; Liva, S. G.; Wang-Lin, S. X.; Kudgus-Lokken, R.; Vermeulen, A.; Ouellet, D. Development of Therapeutic Proteins for a New Subcutaneous Route of Administration After the Establishment of Intravenous Dosages: A Systematic Review. *Clin. Pharmacol. Ther.* **2023**, *113* (5), 1011−1029.
(20) Friedrich, M.; Aigner, A. Therapeutic siRNA: State-of-the-Art and Future Perspectives. *BioDrugs* **2022**, *36* (5), 549−571.
(21) Kulkarni, J. A.; Witzigmann, D.; Thomson, S. B.; Chen, S.; Leavitt, B. R.; Cullis, P. R.; van der Meel, R. The Current Landscape of Nucleic Acid Therapeutics. *Nat. Nanotechnol.* **2021**, *16* (6), 630−643.
(22) Kang, C. Avacincaptad Pegol: First Approval. *Drugs* **2023**, *83* (15), 1447−1453.
(23) Rohner, E.; Yang, R.; Foo, K. S.; Goedel, A.; Chien, K. R. Unlocking the Promise of mRNA Therapeutics. *Nat. Biotechnol.* **2022**, *40* (11), 1586−1600.
(24) Hoy, S. M. Patisiran: First Global Approval. *Drugs* **2018**, *78* (15), 1625−1631.
(25) Scott, L. J. Givosiran: First Approval. *Drugs* **2020**, *80* (3), 335−339.
(26) Scott, L. J.; Keam, S. J. Lumasiran: First Approval. *Drugs* **2021**, *81* (2), 277−282.
(27) Lamb, Y. N. Inclisiran: First Approval. *Drugs* **2021**, *81* (3), 389−395.
(28) Keam, S. J. Vutrisiran: First Approval. *Drugs* **2022**, *82* (13), 1419−1425.
(29) Syed, Y. Y. Nedosiran: First Approval. *Drugs* **2023**, *83* (18), 1729−1733.
(30) Moon, I. J.; Yoon, H. K.; Kim, D.; Choi, M. E.; Han, S. H.; Park, J. H.; Hong, S. W.; Cho, H.; Lee, D.-K.; Won, C. H. Efficacy of Asymmetric siRNA Targeting Androgen Receptors for the Treatment of Androgenetic Alopecia. *Mol. Pharmaceutics* **2023**, *20* (1), 128−135.
(31) *A. Multi-Centre, Randomized, Double-Blind, Placebo-Controlled, Single Ascending Dose Phase 1 Study to Evaluate the Safety, Tolerability and Pharmacokinetics of OLX72021 in Healthy Males with Androgenetic Alopecia*. ACTRN12623000117617 2025(accessed 2025−02−15).
(32) Guo, S.; Li, K.; Hu, B.; Li, C.; Zhang, M.; Hussain, A.; Wang, X.; Cheng, Q.; Yang, F.; Ge, K.; Zhang, J.; Chang, J.; Liang, X.-J.; Weng, Y.; Huang, Y. Membrane-Destabilizing Ionizable Lipid Empowered Imaging-Guided siRNA Delivery and Cancer Treatment. *Exploration* **2021**, *1* (1), 35−49.
(33) An, G. Pharmacokinetics and Pharmacodynamics of GalNAc-Conjugated siRNAs. *J. Clin. Pharmacol.* **2024**, *64* (1), 45−57.
(34) Brown, K. M.; Nair, J. K.; Janas, M. M.; Anglero-Rodriguez, Y. I.; Dang, L. T. H.; Peng, H.; Theile, C. S.; Castellanos-Rizaldos, E.; Brown, C.; Foster, D.; Kurz, J.; Allen, J.; Maganti, R.; Li, J.; Matsuda, S.; Stricos, M.; Chickering, T.; Jung, M.; Wassarman, K.; Rollins, J.; Woods, L.; Kelin, A.; Guenther, D. C.; Mobley, M. W.; Petrulis, J.; McDougall, R.; Racie, T.; Bombardier, J.; Cha, D.; Agarwal, S.; Johnson, L.; Jiang, Y.; Lentini, S.; Gilbert, J.; Nguyen, T.; Chigas, S.; LeBlanc, S.; Poreci, U.; Kasper, A.; Rogers, A. B.; Chong, S.; Davis, W.; Sutherland, J. E.; Castoreno, A.; Milstein, S.; Schlegel, M. K.; Zlatev, I.; Charisse, K.; Keating, M.; Manoharan, M.; Fitzgerald, K.; Wu, J.-T.; Maier, M. A.; Jadhav, V. Expanding RNAi Therapeutics to Extrahepatic Tissues with Lipophilic Conjugates. *Nat. Biotechnol.* **2022**, *40* (10), 1500−1508.
(35) Hsieh, A. C.; Bo, R.; Manola, J.; Vazquez, F.; Bare, O.; Khvorova, A.; Scaringe, S.; Sellers, W. R. A Library of siRNA Duplexes Targeting the Phosphoinositide 3-kinase Pathway: Determinants of Gene Silencing for Use in Cell-based Screens. *Nucleic Acids Res.* **2004**, *32* (3), 893−901.
(36) Wei, N.; Zhang, L.; Huang, H.; Chen, Y.; Zheng, J.; Zhou, X.; Yi, F.; Du, Q.; Liang, Z. siRNA Has Greatly Elevated Mismatch Tolerance at 3′-UTR Sites. *PLoS One* **2012**, *7* (11), No. e49309.
(37) Yoo, M.-H.; Xu, X.-M.; Turanov, A. A.; Carlson, B. A.; Gladyshev, V. N.; Hatfield, D. L. A New Strategy for Assessing Selenoprotein Function: siRNA Knockdown/Knock-in Targeting the 3′-UTR. *RNA* **2007**, *13* (6), 921−929.
(38) Gu, B.; Zeng, X.; Gong, M.; Li, X.; Yu, Q.; Tan, Z.; Lou, Z.; Jiang, T.; Che, Y.; Ao, Y.; Zhu, Y. Target Reprogramming the 3′UTR of Tumor-Suppressor Genes by a siRNA Composite Nanoparticle for Glioblastoma Therapy. *Adv. Funct. Mater.* **2024**, *34* (30), 2400837.
(39) Perez-Mendez, M.; Zárate-Segura, P.; Salas-Benito, J.; Bastida-González, F. siRNA Design to Silence the 3 ′UTR Region of Zika Virus. *BioMed. Res. Int.* **2020**, *2020* (1), 6759346.
(40) Premanand, A.; Reena Rajkumari, B. Androgen Modulation of Wnt/β-Catenin Signaling in Androgenetic Alopecia. *Arch. Dermatol. Res.* **2018**, *310* (5), 391−399.
(41) German, C. A.; Shapiro, M. D. Small Interfering RNA Therapeutic Inclisiran: A New Approach to Targeting PCSK9. *BioDrugs* **2020**, *34* (1), 1−9.

https://doi.org/10.1021/acs.jmedchem.5c01739
J. Med. Chem. 2025, 68, 20586−20594